A R C H I V E S O F M E T A L L U R G Y A N D M A T E R I A L S
Volume 56 2011 Issue 4
DOI: 10.2478/v10172-011-0108-7

J. BIDULSKÁ*, I. POKORNÝ*, T. KVAČKAJ*, R. BIDULSKÝ**, M. ACTIS GRANDE**

STUDY OF THE HIGH-TEMPERATURE BEHAVIOUR OF ALUMINIUM ALLOY EN AW 2014

WYSOKOTEMPERATUROWE ZACHOWANIE STOPU ALUMINIUM EN AW 2014

The high-temperature behaviour of aluminium alloy EN AW 2014 was investigated in a wide range of deformation temperatures and strain rates. The influence of strain rate and temperature on the peak stress was analysed using the conventional constitutive equation (relating strain rate, flow stress, and temperature) and by means of precise definition of the peak stress value, in the non-linear regression model. Moreover, a study on apparent activation energy of EN AW 2014 stabilized by zirconium was carried out using Arrhenius-type plot. The stress-strain curves exhibit rapid increase up to the peak value followed by a gradual softening up to the material fracture, without the steady state usually observed before the fracture. In terms of formability maps, the presented experimental results exhibit a decrease of ductility, respectively with an increase of strain rate and a decrease of temperature, respectively.

Keywords: aluminium alloy, flow stress, constitutive equation, hot working

Wysokotemperaturowe zachowanie stopu aluminium EN AW 2014 badane było w szerokim zakresie temperatur i prędkości odkształcenia. Wpływ prędkości odkształcenia i temperatury na maksymalne naprężenie analizowany był z użyciem konwencjonalnego podstawowego równania (wiążącego prędkość odkształcenia, naprężenie płynięcia i temperaturę) oraz za pomocą precyzyjnej definicji wartości maksymalnego naprężenia w modelu regresji nieliniowej. Ponadto, analiza obserwowanej energii aktywacji stopu EN AW 2014 stabilizowanego cyrkonem przeprowadzono z użyciem wykresu typu Arrheniusa. Krzywe naprężenie-odkształcenie wykazują gwałtowny wzrost do maksymalnego naprężenia, po którym następuje stopniowe miękniecie aż do zerwania materiału, bez obszaru stałego zwykle obserwowanego przed zerwaniem. Jeśli chodzi o mapy plastyczności, przedstawione wyniki doświadczalne wykazują spadek plastyczności, odpowiednio ze wzrostem szybkości odkształcenia oraz ze spadkiem temperatury.

1. Introduction

Mathematical modelling and numerical analysis [1-3] are a proven and reliable technique for analyzing various forming processes [4-7], including flow behaviour during hot deformation condition, in order to analyze the global and local deformation response of the microstructure related to the loading and material properties, to compare the effects of various parameters like strain rates ($\dot{\varepsilon}$) and temperatures (T), and to search for optimum process conditions for a given material.

In general, aluminium alloys represent widely-used materials in aircraft, aerospace, automotive and aeronautical industry due to low density and high strength [8-12].

The hot deformation behaviour of aluminium and its alloys [13-18] has been investigated, particularly with regard to the influence of T and $\dot{\varepsilon}$ on flow stress (σ) and ductility. The results have also been correlated to the typical microstructural characteristics of the investigated alloys.

Several approaches, in combination with shear-line calculations, mathematical modelling and numerical analysis, can be adopted for the evaluation of hot workability, with the aim of predicting the precise relationships among T, $\dot{\varepsilon}$ and deformation (ε) and their influence on σ and microstructure. It is common to make tests keeping T and $\dot{\varepsilon}$ as constant [19-26].

In the present study, the conventional constitutive equation relating $\dot{\varepsilon}$, σ, and T is presented. A subsequent study on the stress-strain ($\sigma - \varepsilon$) behaviour of the material, in terms of precise definition of the σ_p value was carried out in the non-linear regression model. Moreover the apparent activation energy of the investigated mate-

* TECHNICAL UNIVERSITY OF KOŠICE, FACULTY OF METALLURGY, DEPARTMENT OF METALS FORMING, LETNÁ 9, 042 00 KOŠICE, SLOVAKIA
** POLITECNICO DI TORINO-ALESSANDRIA CAMPUS, V. T. MICHEL 5, 15100 ALESSANDRIA, ITALY

rial has been calculated by means of an Arrhenius type constitutive equation.

2. Material and experimental methods

Table 1 shows the chemical composition (wt. %) of the EN AW 2014.

TABLE 1
Chemical composition of investigated alloys /wt. %

Al	Cu	Mn	Si	Mg	Fe	Zr	Ti
Bal.	4.32	0.77	0.68	0.49	0.29	0.13	0.03

Specimens with diameter of 10 mm and length of 20 mm were machined from extruded rods. The torsion test was performed on a computer-controlled torsion machine at the temperature T = 573, 623, 673 and 723 K measured by a K-type thermocouple. After an induction heating in air with a heating rate of 1 K·s^{-1} and a time holding (t) of 180 s^{-1}, the samples fixed in an axial direction were deformed to the fracture at $\dot{\varepsilon}$ of 0.001, 0.01, 0.1, 1 and 5 s^{-1} and water-quenched immediately after the deformation. After rupture, samples were quenched with water jets to avoid microstructure modifications during slow cooling from the testing temperature. Final deformation related to a number of twists to the fracture (N) during the continuous test provides information on formability.

The $\sigma - \varepsilon$ dependence to the strain ε and the strain rate $\dot{\varepsilon}$ was carried out with regard to an analytical-experimental model presented in [17, 26] according to the Von Mises criterion:

$$\sigma = \frac{\sqrt{3}.M_k}{2.\pi.r^3}.(3 + \hat{m} + \hat{n}) \tag{1}$$

where:
σ [MPa] is the flow stress,
M_k [N·mm] is the torque,
r [mm] is the radius of the sample
$\hat{m}$, $\hat{n}$ [-] are coefficients,

$$\varepsilon = \frac{2.\pi.r.N}{\sqrt{3}.L}, \dot{\varepsilon} = \frac{2.\pi.r}{\sqrt{3}.L}\frac{\partial N}{\partial t} \tag{2}$$

where:
N [-] is the number of twists to the fracture,
L [mm] is the length of the sample
and the coefficients $\hat{m}$ and $\hat{n}$ have the forms

$$\hat{m} = \left.\frac{\partial(\ln M_k)}{\partial(\ln \dot{\varepsilon})}\right|_{\varepsilon,T}, \hat{n} = \left.\frac{\partial(\ln M_k)}{\partial(\ln \varepsilon)}\right|_{\dot{\varepsilon},T} \tag{3}$$

where:
$\dot{\varepsilon}$ [s^{-1}] is the strain rate,
ε [-] is the strain,
In steady state or at the peak $\hat{n}$ = 0. Linear up to very high strain rates for both compression and the value of $\hat{m}$ is also usually taken equal to zero.

The method of least squares was used for fitting a function to a set of points from $\sigma - \varepsilon$ curves.

3. Experimental results

3.1. Hot working of investigated aluminium alloys

According to Fig. 1 a-d, the characteristics of aluminium alloy EN AW 2014 $\sigma - \varepsilon$ curves are represented as follows: the $\sigma - \varepsilon$ curves exhibit rapid increase up to the peak value followed by a gradual softening up to the material fracture, without the steady state usually observed before the fracture.

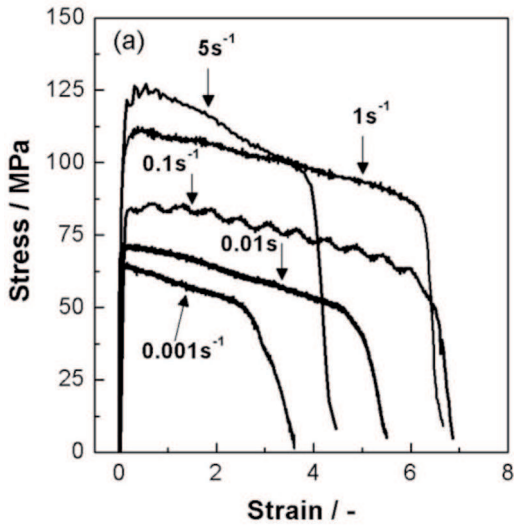

Fig. 1a Stress-strain curves at temperature of 573 K

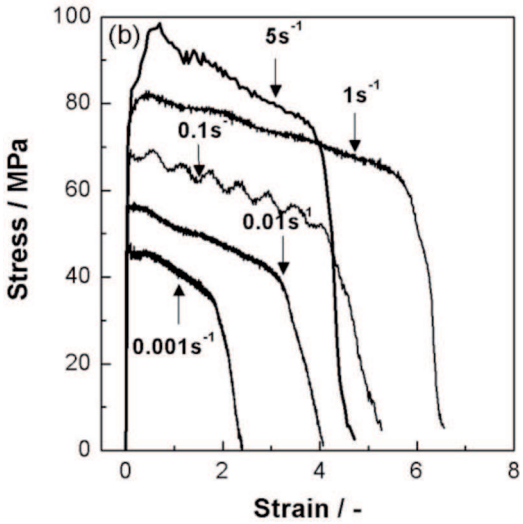

Fig. 1b Stress-strain curves at temperature of 623 K

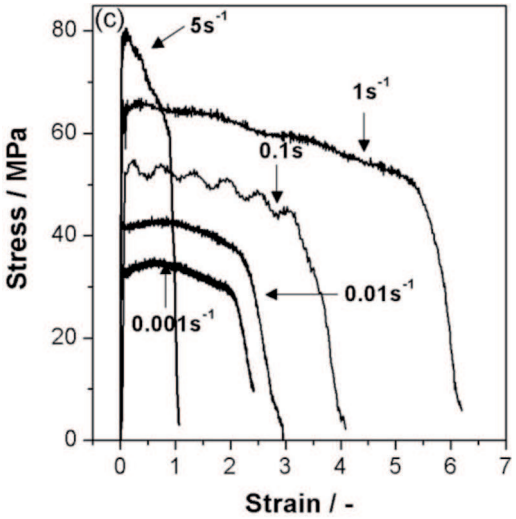

Fig. 1c Stress-strain curves at temperature of 673 K

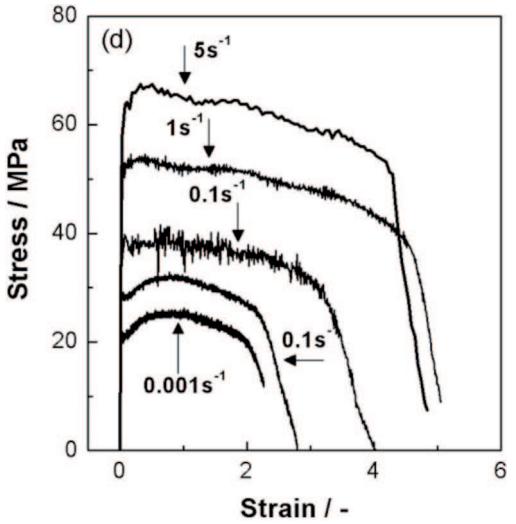

Fig. 1d Stress-strain curves at temperature of 723 K

In the low-temperature regime, the investigated aluminium alloy is characterized by higher σ_p and, after the peaks, by a continuously decaying flow curve. Rupture in general occurs before the σ has reached the steady-state value, this behaviour is typically connected to the over-aged material [27]; at the highest $\dot{\varepsilon}$, material exhibits a continuous decrease in σ, an effect that can be attributed to adiabatic heating. Therefore, microstructural softening plays an important role, which is presented later in detail.

During hot working, concurrent strain hardening and flow softening are commonly observed. In general, a complete material description in terms of σ depends on T, ε and $\dot{\varepsilon}$. Consequently, some investigators have developed constitutive equations for σ based on metallurgical factors [19, 23, 26] known as the sinh law:

$$Z = \dot{\varepsilon} \cdot \exp\left(\frac{-Q_{HW}}{R \cdot T}\right) = A \cdot \left(\sinh\left(\alpha\sigma_p\right)\right)^n \qquad (4)$$

where:

Z [s^{-1}] is the temperature-compensated strain rate, the Zener–Hollomon parameter,

Q_{HW} [$kJ \cdot mol^{-1}$] is the effective activation energy for deformation,

R [$J \cdot mol^{-1} \cdot K^{-1}$] is the gas constant,

T [K] is the temperature,

A [s^{-1}], α [MPa^{-1}] and n [-] are the material constants,

σ_p [MPa] is the peak stress.

In this semi-empirical model the parameters have obvious physical meanings and can be determined easily. Thus, this model is adopted as a general equation of hot working; the strain is represented by steady-state stress. Z is the Zener-Hollomon parameter embracing hot working control variable T, and $\dot{\varepsilon}$. Hot working range requires an additional equation to define that dependence. It will be employed later for comparing different alloys across a wide $\dot{\varepsilon}$ range (0.001 s^{-1} - 10 s^{-1}). The stress multiplier is selected as relative to the range of stresses observed, so that the products with σ give rise to the linear range of the sinh function [23]. It can usually be maintained the same for a group of similar aluminium alloys (α = 0.052 MPa^{-1} [12-19]) and thus permits comparison of the dependence of n and Q_{HW} on composition and microstructure [23].

3.2. Peak stress value derived by a mathematical model

The validity of data regarding activation energy derived from Arrhenius plot, coupled to the assumption that microstructure remains constant, has been debated in different works [14, 15, 18, 23, 28, 29]; the deformation heating tends to reduce the σ at low T leading to a reduced Q. There is the problem of defining the strain at which the value of Q is determined. For aluminium alloys, which ideally harden to a steady state regime as a result of dynamic recovery, it is the plateau stress which could be taken at fixed σ_{ss} (starting at ε_{ss}). Since this may not be precisely attained or there may be some softening due to morphological evolution, it is usual to use the σ_p. Therefore, a subsequent study on the $\sigma - \varepsilon$ behavior of the material in the non-linear regression model was carried out due to a scatter of σ_p values, thus avoiding any problems with identifying a precise value of stress.

The method of least squares was used for achieving non-linear regression equation, basing on the experimental results of torsion test [30, 31]. Correlation index I,

was taken to determine the suitability of non linear regression in describing the $\sigma - \varepsilon$ curve.

The $\sigma - \varepsilon$ curves were analysed by means of non-linear regression model using the method of least squares:

$$\sigma = a_1 + a_2 \cdot \varepsilon - \frac{a_3}{(\varepsilon + a_4)^{a_6} \cdot (a_5 - \varepsilon)^{a_7}} \quad (5)$$

where:

a_1 to a_7 [-] are variable regression parameters.

Non-linear regression models of $\sigma - \varepsilon$ curves describe changes of deformation behaviour up to zero value of stress, considering the variable parameter a_1 as:

$$a_1 = \frac{a_3}{(a_4)^{a_6} \cdot (a_5)^{a_7}} \quad (6)$$

Table 2 presents the calculated values for given T and $\dot{\varepsilon}$.

The value of correlation index I is in the range of 0.827 to 0.998. The experimental and calculated values of aluminium alloy EN AW 2014 stabilized by zirconium is presented in Table 3.

Comparison between experimental and calculated values is presented in the Fig. 2. It can be found that the precise description of the experimental $\sigma - \varepsilon$ curve by means of an analytical model was achieved. Precise values of σ_p were therefore obtained.

TABLE 2

The calculated value for given temperatures and strain rates

T/K	$\dot{\varepsilon}/s^{-1}$	a_1	a_2	a_3	a_4	a_5	a_6	a_7	I
573	**5**	132	-8.39	1649	0.145	5.03	3.18	5.37	0.987
573	**1**	114	-3.95	1649	0.106	7.11	3.07	4.87	0.993
573	**0.1**	89	-3.75	1649	0.078	7.71	2.02	3.95	0.996
573	**0.01**	74	-4.89	1649	0.007	6.71	1.43	5.31	0.998
573	**0.001**	66	-4.96	1649	0.001	5.16	0.84	5.29	0.983
623	**5**	100	-6.39	1649	0.147	5.05	3.81	6.25	0.944
623	**1**	84	-3.22	1649	0.050	7.37	2.00	4.50	0.995
623	**0.1**	71	-3.78	1649	0.004	6.58	0.97	4.48	0.993
623	**0.01**	59	-4.96	1649	0.003	5.88	0.88	4.84	0.975
623	**0.001**	50	-4.95	1649	0.001	4.18	0.66	5.50	0.991
673	**5**	82	-4.12	1649	0.025	6.32	1.44	4.51	0.993
673	**1**	68	-2.64	1649	0.023	7.24	1.63	4.74	0.987
673	**0.1**	57	-3.28	1649	0.076	5.20	1.86	4.95	0.971
673	**0.01**	47	-2.49	1649	0.003	4.64	0.78	5.27	0.982
673	**0.001**	38	-2.49	1649	0.001	4.64	0.56	5.27	0.925
723	**5**	69	-2.32	1649	0.022	6.07	1.43	4.80	0.984
723	**1**	55	-2.18	1649	0.019	6.34	1.50	5.05	0.985
723	**0.1**	44	0.27	1649	0.004	5.72	0.55	3.85	0.987
723	**0.01**	33	-0.27	1649	0.004	4.63	0.70	5.10	0.99
723	**0.001**	28	-2.45	1649	0.010	4.75	0.91	5.30	0.827

TABLE 3

The experimental and calculated values of aluminium alloy 2014

		Experimental values				Calculated values	
						$\sigma = a_1 + a_2 \cdot \varepsilon - \frac{a_3}{(\varepsilon+a_4)^{a_6}\cdot(a_5-\varepsilon)^{a_7}}$	
T/K	$\dot{\varepsilon}$/ **s**$^{-1}$	σ_p/**MPa**	ε_p/–	**N**$_{lom}$/-	ε_{lom}/–	σ_P/**MPa**	ε_P/–
573	**5**	127.1	0.56	2.18	3.95	125.5	0.46
573	**1**	112.5	0.38	3.46	6.27	110.9	0.48
573	**0.1**	86.0	0.61	3.48	6.30	85.6	0.73
573	**0.01**	71.5	0.18	2.59	4.70	72.1	0.19
573	**0.001**	66.0	0.07	1.55	2.80	63.3	0.18
623	**5**	91.7	0.65	2.21	4.00	96.3	0.42
623	**1**	83.0	0.43	3.25	5.88	81.4	0.47
623	**0.1**	69.4	0.10	2.31	4.20	67.9	0.35
623	**0.01**	57.3	0.17	1.82	3.30	55.7	0.15
623	**0.001**	47.8	0.03	1.49	2.60	46.9	0.19
673	**5**	80.6	0.49	2.44	4.42	79.0	0.44
673	**1**	66.9	0.34	3.01	5.46	65.9	0.37
673	**0.1**	54.8	0.23	1.80	3.27	53.5	0.59
673	**0.01**	43.8	0.57	1.27	2.30	44.1	0.30
673	**0.001**	35.8	0.62	1.10	2.00	35.6	0.20
723	**5**	67.4	0.33	2.39	4.34	66.5	0.46
723	**1**	54.6	0.18	2.54	4.61	53.7	0.39
723	**0.1**	41.2	0.53	1.66	3.00	40.0	0.67
723	**0.01**	32.8	0.78	1.19	2.15	31.4	0.60
723	**0.001**	26.3	1.01	1.05	1.90	25.5	0.33

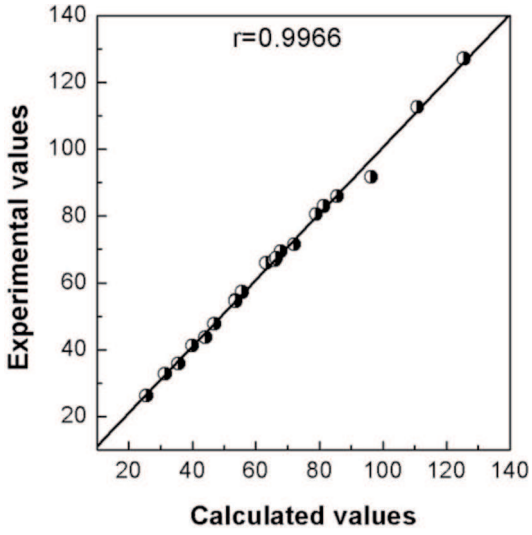

Fig. 2. Comparison between experimental and calculated values of σ_p

The σ_p dependence on $\dot{\varepsilon}$ of aluminium alloys has usually been described [14, 15, 18, 23, 28, 29] by the expression:

$$\dot{\varepsilon} = A \cdot \left(\sinh \alpha\sigma_p\right)^n \exp\left(\frac{-Q_{HW}}{R \cdot T}\right) \tag{7}$$

The Q_{HW} was obtained from the slope S in an Arrhenius type plot by the equation:

$$Q_{HW} = 2.3 \cdot n \cdot R \cdot S \tag{8}$$

Fig. 3 and Fig. 4 shows the plots used to calculate the average values of n (n_{avg}) and S (S_{avg}), being α =0.025 MPa^{-1} as the "traditional" value for aluminium alloys [14, 15, 18, 23, 27-29].

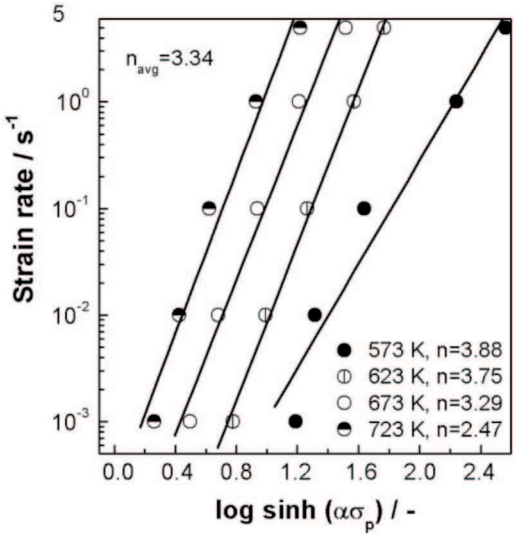

Fig. 3. Plot used for the calculation of of n (n_{avg}), being α =0.025 MPa^{-1}

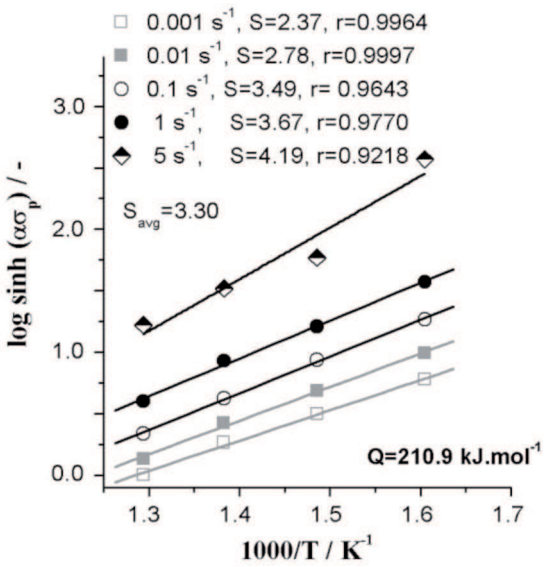

Fig. 4. Plot used for calculating the S (S_{avg}), being α =0.025 MPa^{-1} and therefore achieving the apparent activation energy

The activation energy was than achieved. This value for hot working deformation is relatively close to the activation energy of 200 kJ·mol^{-1} and especially, when an investigation of its hot formability by torsion tests tested in as-extruded condition [32, 33] or for aluminium alloys of 2XXX series [34, 35].

3.3. Relative softening

The studies of hot workability of aluminium alloys [13, 15, 18, 23, 28, 33] have demonstrated convincingly that high-temperature deformation in these materials is controlled by dynamic softening. As a consequence, the flow curves exhibit strain-hardening to a steady state, even though in certain conditions a moderate peak is observed. Therefore the gradual softening is the result of particle coarsening during high-temperature deformation [34, 36]. Thus, investigated EN AW 2014 aluminium alloys exhibit a high σ_p due to dynamic precipitation, followed by rapid softening as the fine particles coalesce [29].

Additionally, the relative softening (X_{RS} after σ_p, derived as [34, 35]:

$$X_{RS} = \frac{\sigma_p - \sigma_{p+0.25}}{\sigma_p} \tag{9}$$

and shown in Fig. 5 at different T and $\dot{\varepsilon}$, represents an increasing function of T, where $\sigma_{p+0.25}$ is a stress at $\varepsilon = 0.25$ after σ_p.

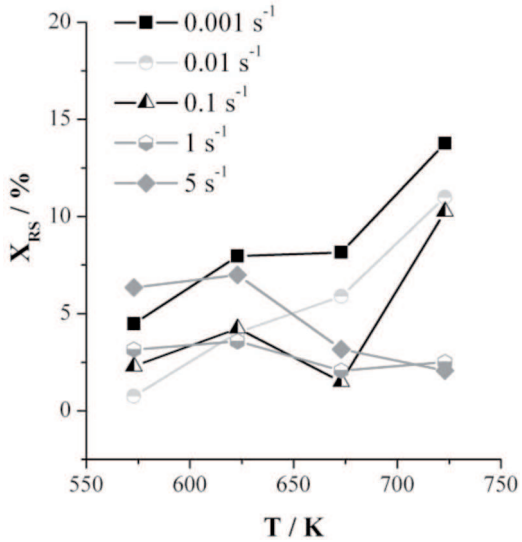

Fig. 5. Curves of relative softening in terms of strain rate and temperature

The X_{RS} is a consequence of dynamic recrystallization and dynamic recovery resulting from a high dislocation density leading to the formation of subgrains. With regard to [34], finer particles to be responsible for higher strength are also able to intensively coalesce to result in intensive softening.

3.4. Hot formability

In general, the fracture strain ε_f is considered to represent the ductility of a material. The relationship $\varepsilon_f = \varepsilon_f(T, \dot{\varepsilon})$ in Fig. 6 exhibits an improvement of ductility with decreasing T and increasing $\dot{\varepsilon}$.

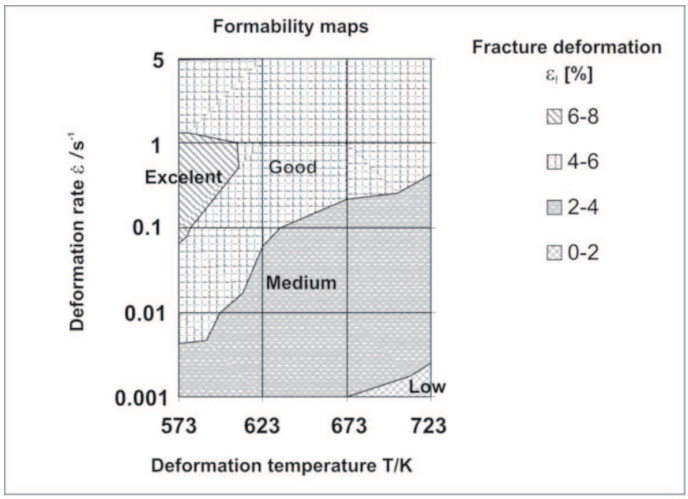

Fig. 6. Formability maps for investigated alloy

The optimal T for the evaluated formability was 573 K. This assumption was confirmed in [37], where similar results recorded at T = 573 K and 623 K. The maximum ductility was recorded at the T = 573 K, the increasing T resulted in the decreased ductility of material.

4. Discussion

Previous works on the aluminium alloy EN AW 2014 [1, 13-16, 27] showed that the microstructure consisted of chains of equiaxed or slightly elongated subgrains that developed inside the elongated grains; TEM inspection revealed the presence of a dispersion of precipitates within the grains. Even at the highest temperature which closely was corresponding to the solution-treatment temperature as stated by thermodynamical calculations of authors [27], the subgrain interior showed a distribution of fine precipitates. Considerable dislocation interaction with all the fine precipitates was also observed, revealing their hardening effect. Therefore, subgrains are larger and more recovered in relation to higher T, lower $\dot{\varepsilon}$ and σ; this behaviour results from dynamic recrystallization and dynamic recovery. Dynamic recrystallization and recovery seems to be occur [38] but its uniformity after monotonic hardening to steady state greatly enhances the ductility. Additionally, the TEM inspection [27] clearly and exhaustively showed the pinning effect of the Al_3Zr dispersoids both on the grain-boundary migration and on the subgrain sliding.

Considering that the sinh constitutive analysis is frequently related to the σ_p as being indicative of the maximum stress occurring in a process with defined T and $\dot{\varepsilon}$ [39], the main aim of the presented investigation was to find solution of precise definition. However, the analysis could be for stress at a constant strain that is related to the process range. The yield point is not usually employed since it is difficult to define at high T, and is far below the typical values of ε and σ in industrial forming. The softening behaviour of the studied aluminium alloy can be modelled with an $\varepsilon-$ independent σ; according to [18, 23, 35] this is generally suitable for aluminium alloys with dynamic recrystallization and recovery plateaus. Optimizing all the material constants can marginally raise the correlation coefficient but this often results in large variations in Q_{HW} and n that cannot be related to alloying additions or microstructures. In aluminium alloys with the mechanism being solely dynamic softening, the Q_{HW} range is much broader rising higher above Q_D (as diffusion, which is determined by power law, especially in the creep condition) as the alloying and the impurity content (mainly particles) rises [13-15,18, 23, 39-42].

In order to verify the developed non-linear regression model, the error between the calculated σ_p ($\sigma_p\,(calculated)$) and experimentally obtained σ_p ($\sigma_p\,(experimental)$) was calculated:

$$error = \frac{\sigma_p\,(calculated) - \sigma_p\,(experimental)}{\sigma_p\,(calculated)} \cdot 100\ \% \tag{10}$$

The Table 4 shows the error results in the range from 0.47 to 5.02 %. The average values of errors are 1.62 %, 2.76 %, 1.42 % and 2.64 % for T = 573 K, 623 K, 673 K and 723 K, respectively.

TABLE 4

The validation of proposed non-linear model

T/K	$\dot{\varepsilon}$/s^{-1}	$\sigma_p\,(calculated)$/MPa	$\sigma_p\,(experimental)$/MPa	Error/%	Avg. error/%
573	**5**	127.1	125.5	1.26	
573	**1**	112.5	110.9	1.42	
573	**0.1**	86.0	85.6	0.47	**1.62**
573	**0.01**	71.5	72,1	0,84	
573	**0.001**	66.0	63.3	4.09	
623	**5**	91.7	96.3	5.02	
623	**1**	83.0	81.4	1.93	
623	**0.1**	69.4	67.9	2.16	**2.76**
623	**0.01**	57.3	55.7	2.79	
623	**0.001**	47.8	46.9	1.88	
673	**5**	80.6	79.0	1.99	
673	**1**	66.9	65.9	1.49	
673	**0.1**	54.8	53.5	2.37	**1.42**
673	**0.01**	43.8	44.1	0.68	
673	**0.001**	35.8	35.6	0.56	
723	**5**	67.4	66.5	1.34	
723	**1**	54.6	53.7	1.65	
723	**0.1**	41.2	40.0	2.91	**2.64**
723	**0.01**	32.8	31.4	4.27	
723	**0.001**	26.3	25.5	3.04	

5. Conclusions

(1) Every stress-strain curve shows a rapid increase in the stress to a peak value, followed by a gradual decrease towards a steady state regime which is not reached.
(2) A subsequent study on the stress-strain behaviour of the material in the non-linear regression model was carried out due to a scatter of peak stress values, thus avoiding any problems with identifying a precise value of stress.
(3) The apparent activation energy of aluminium alloy EN AW 2014 stabilized by zirconium has been determined.
(4) The relative softening is a consequence of dynamic recrystallization and recovery deriving from stress-strain curves was determined.
(5) Optimal values of hot formability $\dot{\varepsilon}$ = 0.001 s^{-1}, T = 573 K with regard to the ductility are thus obtained.

Acknowledgements

J. Bidulská thanks the bilateral project SK-PL-0011-09. R. Bidulský thanks the Politecnico di Torino and the Regione Piemonte for co-funding the fellowship. We also thank Dr. F. Bardi for technical assistance at torsion test. This work was realized within the frame of the project "Technological preparation of electrotechnical steels with high permeability for electrodrives with higher efficiency", which is supported by the Operational Program "Research and Development" ITMS 26220220037, financed through European Regional Development Fund.

REFERENCES

[1] J. Bidulská, T. Kvačkaj, R. Kočiško, R. Bidulský, M. Actis Grande: Acta Metallurgica Slovaca **14**, 342-348 (2008).

[2] R. Ebrahimi, S.H. Zahiri, A. Najafizadeh, Journal of Materials Processing Technology **171**, 301-305 (2006).
[3] X. He, Z. Yu, G. Liu, W. Wang, X. Lai, Materials and Design **30**, 166-169 (2009).
[4] R. Bidulský, J. Bidulská, M. Actis Grande: High Temperature Materials and Processes **28**, 337-342 (2009).
[5] M. Kopernik, M. Pietrzyk, Archives of Metallurgy and Materials **52**, 299-310 (2007).
[6] J. Nowak, L. Madej, F. Grosman, M. Pietrzyk, Materials Science Forum **654-656**, 1622-1625 (2010).
[7] M. Kvačkaj, T. Kvačkaj, A. Kováčová, R. Kočiško, J. Bacsó, Acta Metallurgica Slovaca **16**, 84-90 (2010).
[8] J. Bidulská, T. Kvačkaj, R. Bidulský, M. Actis Grande: Kovove Materialy **46**, 339-344 (2008).
[9] J. Bidulská, T. Kvačkaj, R. Bidulský, M. Actis Grande: High Temperature Materials and Processes **27**, 203-207 (2008).
[10] J. Bidulská, I. Pokorný, T. Kvačkaj, R. Bidulský, M. Actis Grande: High Temperature Materials and Processes **28**, 315-321 (2009).
[11] E. Nes, Acta Metallurgica **20**, 499-506 (1972).
[12] J.D. Robson, P.B. Prangnell, Acta Materialia **49**, 599-613 (2001).
[13] J. Bidulská, R. Bidulský, L. Ceniga, T. Kvačkaj, M. Cabibbo, E. Evangelista, Kovove Materialy **46**, 151-155 (2008).
[14] S. Spigarelli, M. Cabibbo, E. Evangelista, J. Bidulská, Journal of Materials Science **38**, 81-88 (2003).
[15] F. Bardi, M. Cabibbo, E. Evangelista, S. Spigarelli, M. Vukcevic, Materials Science and Engineering A **A 339**, 43-52 (2003).
[16] J. Bidulská, T. Kvačkaj, R. Bidulský, M. Cabibbo, E. Evangelista, Metalurgija **46**, 157-159 (2007).
[17] R. Pernis, J. Kasala, J. Bořuta, Acta Metallurgica Slovaca **15**, 5-14 (2009).
[18] H.J. McQueen, Metallurgical and Materials Transactions A **33A**, 345-362 (2002).
[19] J.J. Jonas, C.M. Sellars, W.J.McG. Tegart, International Metallurgical Reviews **14**, 1-24 (1969).
[20] C.M. Sellars, W.J. McG. Tegart, International Metallurgical Reviews **17**, 1-24 (1972).
[21] A.K. Ghosh, Acta Metallurgica **28**, 1443-1465 (1980).
[22] Y. Estrin, H. Mecking, Acta Metallurgica **32**, 57-70 (1984).
[23] H.J. McQueen, N.D. Ryan, Materials Science and Engineering A **A 322**, 43-63 (2002).
[24] Y.V.R.K. Prasad, S. Sasidhara, Hot working guide: A compendium of processing maps, ASM International, Materials Park, (1997).
[25] M.E. Kassner, M.T. Perez-Prado, Progress in Materials Science **45**, 1-102 (2000).
[26] H.J. McQueen, X. Xia, Y. Cui, B. Li, Q. Meng, Materials Science and Engineering A **A 319-321**, 420-424 (2001).
[27] M. Cabibbo, E. Evangelista, S. Spigarelli, Metallurgical and Materials Transactions A **35 A**, 293-300 (2004).
[28] S. Spigarelli, E. Evangelista, H.J. McQueen, Scripta Materialia **49**, 179-183 (2003).
[29] E. Cerri, E. Evangelista, A. Forcellese, H.J. McQueen, Materials Science and Engineering A **A 197**, 181-198 (1995).
[30] A. Ralston, A first course in numerical analysis, Mc Graw – Hill, New York, (1964).
[31] J.L. Buchanan, P.R. Turner, Numerical method and analysis, Mc Graw – Hill, New York, (1992).
[32] S. Spigarelli, F. Bardi, E. Evangelista, Materials Science Forum **331-337**, 449-454 (2000).
[33] F. Bardi, M. Cabibbo, S. Spigarelli, Materials Science and Engineering A **A 334**, 87-96 (2002).
[34] P. Wouters, B. Verlinden, H.J. McQueen, E. Aernoudt, L. Delaey, S. Cauwenberg, Materials Science and Engineering A **A123**, 239-245 (1990).
[35] H.J. McQueen, M.J. Lee, Materials Science Forum **331-337**, 437-442 (2000).
[36] B. Verlinden, P. Wouters, H.J. McQueen, E. Aernoudt, L. Delaey, S. Cauwenberg, Materials Science and Engineering A **A123**, 229-237 (1990).
[37] E. Evangelista, in Hot deformation of aluminum alloys, eds. T.D. Langdon, H.D. Merchant, J.G. Morris and M.A. Zaidi, Minerals, Metals and Materials Society, Warrendale, 121 (1991).
[38] S. Spigarelli, M. El Mehtedi, E. Evangelista, J. Kaneko, Materials Science and Technology **17**, 627-638 (2001).
[39] H.J. McQueen, P. Leo, E. Cerri, Materials Science Forum **604-605**, 53-65 (2009).
[40] H.J. McQueen, D.L. Bourell, Journal of Materials Shaping and Technology **5**, 53-73 (1987).
[41] C. Huang, E.B. Hawbolt, X. Chen, T.R. Meadowcroft, D.K. Matlock, Acta Materialia **49**, 1445-1452 (2001).
[42] K. Nagyová, M. Fujda, P. Horňak, In: Metalurgia Junior 2008, Košice: HF TU, ISBN 9788055300375, 139-142 (2008).

Received: 15 April 2011.